T-matrix approach for the calculation of local fields in the neighborhood of small clusters in the electrodynamic regime

Luis Cruz
Department of Physics, University of Puerto Rico, P.O. Box 23334, University Station, Rio Piedras, Puerto Rico 00931-3334

Luis F. Fonseca
Escuela de Física, Universidad de Costa Rica, San Jose, Costa Rica

Manuel Gómez
Department of Physics, University of Puerto Rico, P.O. Box 23334, University Station, Rio Piedras, Puerto Rico 00931-3334
(Received 18 January 1989; revised manuscript received 19 April 1989)

The *T*-matrix formalism developed by Waterman and extended to clusters by Peterson and Ström is used to calculate local electric fields for single spherical and spheroidal metallic particles as well as for two-particle clusters. The calculations are done in the electrodynamic regimes as well as in the long-wavelength regime. Radial dependence, angular distributions, and multipolar composition of resonances are analyzed for all cases. Comparison with calculations of local fields by recent electrostatic formulations of the problem are performed. The failure of the multiple-scattering approach for clusters with scatterers in close proximity in the long wavelength regime is discussed. The existence of a critical interparticle distance at which occurs a maximum enhancement for clusters of two ellipsoidal particles is obtained. The versatility of the *T*-matrix method for calculating the local field in the neighborhood of clusters made up of arbitrary scatterers is demonstrated.

INTRODUCTION

Although the interaction of the electromagnetic radiation with particulate matter has been studied for a long time,[1,2] clustering effects in the electrodynamic regime are not yet well understood. New and increased interest has developed in this subject due to the fact that clustering is essential to the understanding of many physical processes of interest, such as surface-enhanced Raman scattering, as well as light scattering and absorption from metallic colloids in alkali halide crystals.[3–8]

Isolated spheres and spheroids in the long-wavelength regime, that is, when the incident wavelength is much larger than the size of the particle, as well as in the electrodynamic regime, where the particle is comparable to the incident wavelength, have been analyzed in the radiation zone.[9–12] Studies restricted to the surface of the scattering particles have also been done.[13] Clusters of spheres have been analyzed, but mainly in the radiation zone[14–17] or using an electrostatic approach.[18]

The purpose of this work is to present the results of detailed and comprehensive calculations of the scattered electric field in the vicinity of isolated and clusters of metallic scatterers. The calculations are done with an electrodynamic approach that considers vectorial multipolar fields, in contrast to other recent electrostatic approaches[15] that consider scalar multipolar potentials. In the long-wavelength regime it is verified that both approaches give similar results. For clusters of spheres and spheroids the calculations have been done in both the long-wavelength as well as the electrodynamic regimes as a function of the separation between the metallic particles and, in the case of ellipsoidal particles, also as a function of relative orientations of the ellipsoids. To the best of our knowledge, no results have been previously published on the local field induced around metallic clusters in the electrodynamic regime.

The method used in this work is the *T*-matrix formalism developed by Waterman.[9] With use of vector spherical partial waves (Ψ_n) as a basis set, a matrix formalism is derived describing electromagnetic scattering for a general wave incident on objects of arbitrary shape. The extension to two scatterers is taken from Peterson and Ström,[14] who developed an effective *T* matrix for more than one scatterer, retaining all the advantages of the Waterman formalism and permitting calculations even when scatterers in the cluster have arbitrary shapes. Although calculations are limited to spherical and slightly ellipsoidal particles and two-particle clusters, general conclusions are given based on the obtained results. As a result of this work it is concluded that in the long-wavelength regime a multiple-scattering expansion for scatterers in close proximity, like those used in Ref. 19, is no longer valid when the frequency of the electric field is near a resonance. Furthermore, it is shown that for clusters a distance greater than the one when the metallic particulates are in contact will give maximum local-field intensity.

For all the calculations in this paper, silver was used as a model metal using the complex frequency-dependent dielectric-function values reported in the literature for the bulk material.[20]

Section I of this article deals with the *T*-matrix formalism applied to isolated spherical and ellipsoidal particles. In the long-wavelength regime previous work using an electrostatic approach is corroborated, and the formalism is extended to larger spherical and spheroidal metallic particles where it is necessary to do the calculations in

the electrodynamic regime.

The calculations are done as expansions in spherical harmonics Ψ_n whose number n corresponds to terms in the multipolar expansion. Angular distributions and multipolar composition of the fields in the vicinity of the particle are studied and the radial dependence of the field is analyzed. Expanding the T matrix in spheroidal wave functions would naturally make the T matrix diagonal for ellipsoids, and then only the dipolar term would be important in the long-wavelength regime. Since the main objective of this paper is to study clusters, spherical harmonics prove to be the most convenient base; thus, all calculations are done in terms of this base.

Section II considers the formalism for clusters of two scatterers in both the long-wavelength as well as the electrodynamic regime for spheres. It is shown that a multiple-scattering approach is not feasible when the scatterers are in close proximity, and strongly interacting, explaining divergent results for touching spherical scatterers found in the literature.[19] For these clusters the interesting feature of a maximum local scattered field found at critical interparticle distance greater than that for particles in contact is demonstrated. Furthermore, it is shown that when the interparticle distance of clusters exceeds four particle radii the behavior of the local field at any one of the scatterers is no longer influenced by the other scatterer, thus establishing a criterion for a decoupling distance for cluster effects.

I. SINGLE SCATTERERS

A. The formalism

The T-matrix formalism developed by Waterman[9] takes into account multipolar contributions which are essential for any valid calculation of the local field of single-particle ellipsoids as well as for all clusters. It also fully takes into account phase-retardation effects due to the size of the scatterers which are important for particles and clusters whose sizes are comparable to the wavelength of the incident field. For this reason the formalism has been chosen to calculate local fields near spheres, spheroids, and clusters of two scatterers both in the long-wavelength as well as in the electrodynamic regime.

In this method, the scattered field is obtained in terms of the incident field by expanding the three fields (incident, internal, and scattered) in terms of the corresponding elementary fields that are a basis set of solutions for the vector Helmholtz equation

$$\nabla\times\nabla\times\mathcal{E}-k^2\mathcal{E}=\mathbf{0} .$$

The incident $\mathcal{E}_0$ and the internal $\mathcal{E}_{\rm int}$ are expanded in terms of the regular basis $\mathrm{Re}\Psi$ and the scattered $\mathcal{E}_s$ in terms of the nonregular Ψ one:

$$\mathcal{E}_0=\sum_n A_n \mathrm{Re}\Psi_n ,$$

$$\mathcal{E}_s=\sum_n F_n \Psi_n ,$$

$$\mathcal{E}_{\rm int}=\sum_n D_n \mathrm{Re}\Psi_n .$$

The elementary wave functions are expressed as

$$\Psi_{\tau\sigma mn}(\mathbf{r})=\gamma_{mn}^{1/2}(k^{-1}\nabla\times)^{\tau}[k\mathbf{r}Y_{\sigma mn}(\hat{\mathbf{r}})h_n(kr)]$$

where $\tau=1,2$, $\sigma=$even (e) or odd (o), $n=1,2,\ldots,$ and $m=0,1,\ldots,n$, and

$$\gamma_{mn}=\varepsilon_m\frac{(2n+1)(n-m)!}{4n(n+1)(n+m)!} ;$$

also,

$$Y_{emn}(\hat{\mathbf{r}})=\cos(m\phi)P_n^m(\cos\theta) ,$$

$$Y_{omn}(\hat{\mathbf{r}})=\sin(m\phi)P_n^m(\cos\theta) .$$

$\tau=1,2$ describes the type of excitation—magnetic or electric—ε_m is the Neumann symbol defined as $\varepsilon_0=1$ ($\varepsilon_m=2$ otherwise), n is the order of the multipole, and σ gives the parity of the elementary functions. The regular forms of the basis functions are obtained by substituting the Hankel functions by the Bessel functions.

The surface currents on the scatterers are used to express the expansion coefficients yielding, finally, a relation between the latter:

$$\mathbf{F}=-i\,\mathrm{Re}(\underline{Q}')\mathbf{D} , \tag{1}$$

$$\mathbf{A}=i\underline{Q}'\mathbf{D} , \tag{2}$$

where $\underline{Q}$ represents the transpose of the $\underline{Q}$ matrix which for a particle with complex dielectric function is given by

$$Q_{nn'}=\frac{k_0}{\pi}\int_s ds\cdot\{[\nabla\times\mathrm{Re}\Psi_n(k\mathbf{r})]\times\Psi_{n'}(k_0\mathbf{r}) + \mathrm{Re}\Psi_n(k\mathbf{r})\times[\nabla\times\Psi_{n'}(k_0\mathbf{r})]\} ,$$

where $k_0^2=\varepsilon_{\rm ext}\omega^2/c^2$ and $k^2=\varepsilon_{\rm int}\omega^2/c^2$, s is the surface of the scatterer, and $\Psi_n(k\mathbf{r})$ is substituted by $\mathrm{Re}\Psi_n(k\mathbf{r})$ wherever $\mathrm{Re}Q$ appears. In our case $\varepsilon_{\rm ext}=1$ (vacuum) and $\varepsilon_{\rm int}$ is the corresponding value for silver.

Finally, eliminating $\mathbf{D}$ from Eqs. (1) and (2), a relation between the coefficients of the scattered and incident fields is obtained:

$$\mathbf{F}=\underline{T}\,\mathbf{A} , \tag{3}$$

where $\underline{T}$ is the T matrix of the scatterer defined as

$$\underline{Q}\,\underline{T}=-\mathrm{Re}\underline{Q} .$$

The scattered field can be expressed in terms of the incident field using the T matrix by the following relationship:

$$\mathcal{E}_s=\underline{T}\mathcal{E}_0 .$$

Most of the results presented in this paper will be expressed in terms of the total electric field given by the following:

$$\mathcal{E}_t=\mathcal{E}_s+\mathcal{E}_0 .$$

It is worth noting that the local fields can only be calculated starting from a minimum circumscribing sphere from the scatterer to assure convergence of the spherical-wave expansions.

B. The sphere

1. Long-wavelength regime

The T matrix for spheres is diagonal and yields the same result as the Mie theory. For the case of the incident wavelength much larger than the dimension of the sphere ($a/\lambda \approx 0.01$, where a is the radius of the sphere and λ is the incident wavelength) a dipolar response is obtained as can be predicted directly from the electrostatic equation.[21] In this long-wavelength regime only a surface-plasmon mode of dipolar character is excited. Performed calculations for silver spheres in the range of the incident wavelength of interest (from 300 to 800 nm) yield that for radii less than $a < 5$ nm the dipolar approximation applies.

2. Electrodynamic regime

For spheres in the electrodynamic regime, that is, spheres whose radii are comparable with the incident wavelength ($a/\lambda \approx 0.1$), multipoles higher than the dipole are excited (see, for example, Refs. 22 and 23) and become important for the calculation of local field $r \approx a$, where r is the radius distance from the origin to the point of observation. Calculations using a sphere with a radius of 50 nm indicates that multipoles up to order $n = 9$ have to be considered in order to get a good convergence of the scattered local electric field.

Since for spheres in the electrodynamic regime higher multipoles other than the dipole influence the scattered wave, more than one characteristic peak for the spectrum should be expected and is observed. Figure 1 shows the intensity of the total scattered field as a function of wavelength for three distances of observation from the center of a sphere of radius 50 nm in the x direction. The intensity of the incident wave for all calculations in this paper are taken to be 1. For this particle size, two resonant peaks are observed. The variation of field intensity with observation distance shows that the smaller-wavelength peak falls faster than the other. This, and the fact that the longer-wavelength peak red-shifts (resonant energy for the electrodynamic case $E = 3.12$ eV, $\lambda = 397$ nm; resonant energy for the electrostatic case $E = 3.5$ eV, $\lambda = 354$ nm) yields a lower intensity of the total electric field ($|\mathcal{E}|^2 = 62.41$ for the electrodynamic case, $|\mathcal{E}|^2 = 456.7$ for the electrostatic case), and broadens with respect to the electrostatic case, leads us to assign this peak a dipolar surface-plasmon character, in accord with previous works.[13,16] Martinos,[22] using a Mie formalism, generates high-energy peaks in the absorption cross section for electrodynamic spheres and similarly identifies these as belonging to higher multipoles.

To ascertain further the multipolar character of the peaks, the scattered field is decomposed into its different multipoles for each of the two resonant energies in Fig. 1. This is accomplished by taking into account only specific n's (order of the multipoles) in the coefficients of the scattered field, Eq. (3). For the resonant energy of the scattered wave, $E = 3.12$ eV ($\lambda = 397$ nm), it is found that in the relative contributions of the multipoles to the field, the one with $n = 1$ (the dipole) gives the highest contribution [Fig. 2(a)]; therefore, that peak is denoted as dipolar in character. For the resonant energy of the scattered wave, $E = 3.5$ eV, a similar analysis shows that [Fig. 2(b)] the $n = 2$ multipole (the quadrupolar) dominates over the other multipoles, therefore giving that second peak a quadrupolar character. It is worth noting that since the T

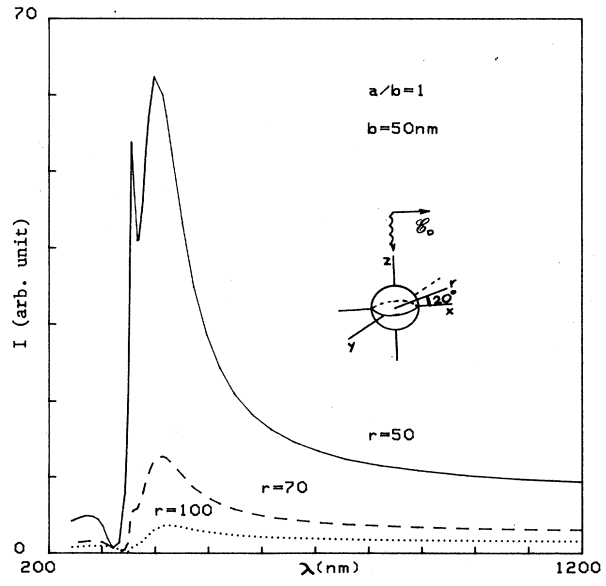

FIG. 1. Total electric field intensity $|\mathcal{E}_t|^2$, at an angle of 70° from the z axis in the x-z plane, as a function of incident wavelength for an electrodynamic sphere, $b = 50$ nm. Three distances of observation are presented, $r = 50$ nm (on the surface) and $r = 70$ and 100 nm.

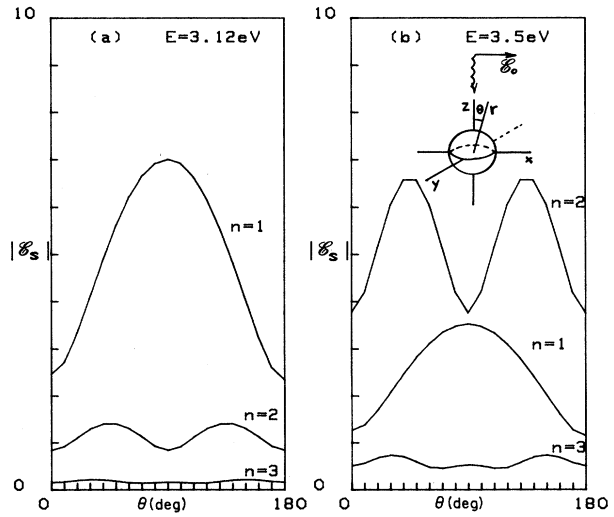

FIG. 2. (a) and (b) Separate multipolar contributions n to the scattered field $\mathcal{E}_s$ for the two resonant energies of Fig. 1, for the sphere $b = 50$ nm. The angle θ is measured from the z axis in the x-z plane.

matrix in Eq. (3) is diagonal, the contributions of each multipole is pure for each n, a fact that is only true for isolated spheres and which will get complicated by nondiagonal terms in the T matrix for ellipsoidal scatterers and for all clusters.

An interesting feature comes out from the calculation of the magnitude of the total field (all n's considered) in the external region of the sphere as a function of its angular position. From Fig. 3 it can be observed [both (a) and (b)] that given a certain angular position on the surface of the sphere, the high-energy peak [$E=3.5$ eV, Fig. 3(b)] has a greater magnitude than the dipolar one [Fig. 3(a)]; therefore, multipolar excitations other than the dipole are as important as the dipole itself in the calculation of maximum intensities of the local fields for spheres of this size. Therefore, the electrodynamic analysis is fundamental in the calculation of the scattered electric field around spheres whose size is comparable with the incident wavelength.

C. The ellipsoid

1. *Long-wavelength regime*

When the particle is ellipsoidal rather than spherical, multipolar contributions become significant in the calculation of the local field even when the size of the particle is small compared to the incident wavelength due to the fact that the expansion of the T matrix is made in terms of spherical wave functions. These multipolar contributions are made important by the appearance of off-diagonal terms in the T matrix which mix the different multipoles of the incident wave. Although these off-diagonal terms are small (no larger than 10^{-8} when compared with diagonal terms), when calculating the field in the local region $r \approx a$ these terms are multiplied by the elementary fields into which the incident plane wave is decomposed [Eq. (3)], and because of the divergent nature of the Neumann functions, the product makes contributions to the scattered field of the same order of magnitude as those coming from diagonal terms. Then, even if the incident field would be purely dipolar, the scattered field would contain elementary fields corresponding to higher-order multipoles, that is, the coefficient of a given elementary field in the scattered field can have contributions from various multipolar terms in the incident wave.

For the specific case of the electric field at the tip of the ellipsoid, with the incident field parallel to the semimajor axis, the T matrix calculations yield the value given for the electrostatic limit found in the literature.[21] In this case, the resonant peak shifts to the red and grows in intensity as the ratio a/b (a is the semiminor axis, b is the semimajor axis) gets smaller, as is predicted by electrostatic theories.

Convergence of the calculations for the intensity of the scattered local field becomes computationally difficult when the ratio a/b is sufficiently different from that of a sphere. For example, for prolate spheroids of $a/b=0.9$ and $b=5$ nm (electrostatic regime), convergence is achieved for the value of the scattered field when $n=7$, while for $a/b=0.8$ and $b=5$ nm it is necessary to go up to $n=9$ to achieve convergence.

Furthermore, it is found that calculations done at the resonant energies for the local field need a higher n in order to obtain convergence, compared to the same calculation done for off-resonant energies. Also, as stated above, to achieve convergence as the ratio a/b decreases, a higher n is required. This is shown graphically in Figs. 4(a) and 4(b). The figures show the relative contributions

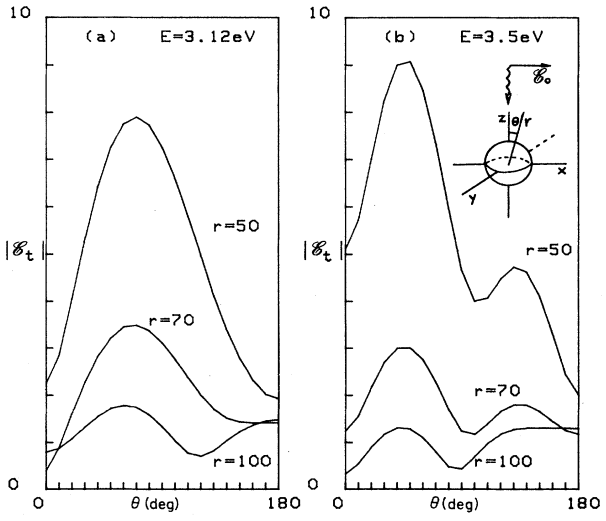

FIG. 3. (a) and (b) Total electric field $\mathscr{E}_t$ as a function of angle from the z axis in the x-z plane, for a sphere of $b=50$ nm. The energies presented correspond to the two resonances of Fig. 1 for three distances of observation ($r=50$, 70, and 100 nm).

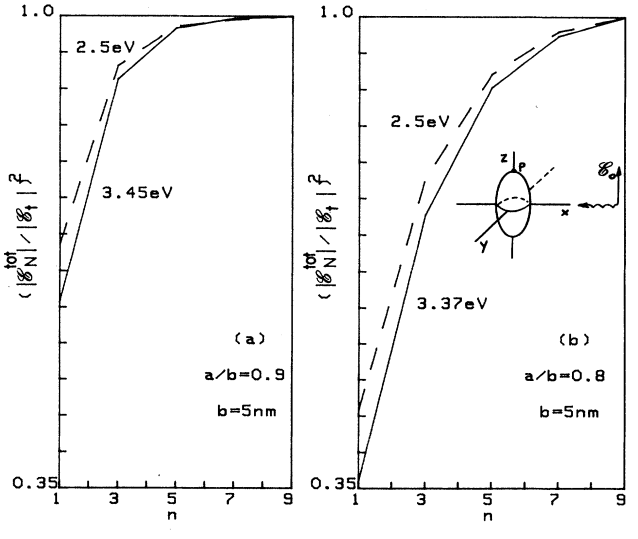

FIG. 4. (a) and (b) Relative multipolar contributions, where $\mathscr{E}_N^{tot}=\sum_{n=1}^{N}\mathscr{E}_n$ is the total electric field considering terms up to order N, (a) for $a/b=0.9$, $b=5$ nm; (b) and $a/b=0.8$, $b=5$ nm. $\mathscr{E}_N^{tot}$ is normalizd by the total electric field $\mathscr{E}_t$. The point P is the observation point.

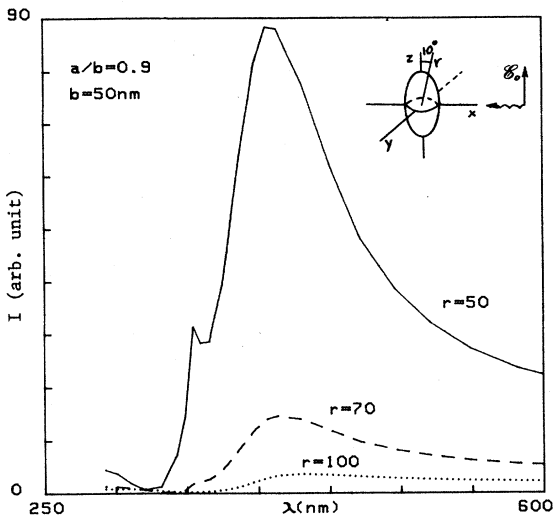

FIG. 5. Total electric field intensity as a function of incident wavelength at an angle of 10° from the z axis in the x-z plane for an ellipsoid with $a/b=0.9$ and $b=50$ nm. Three distances of observation are presented.

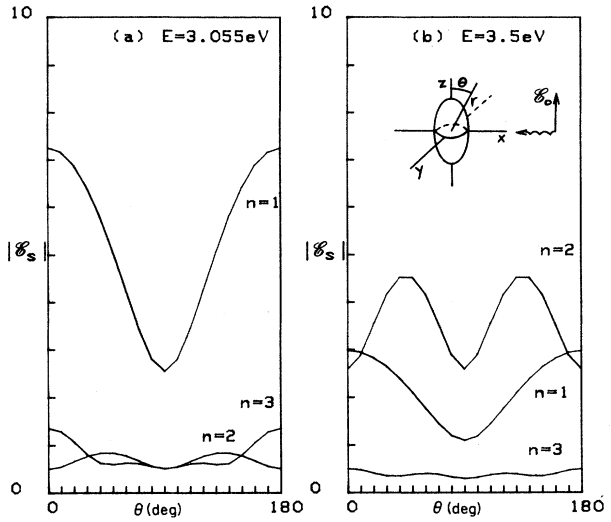

FIG. 6. (a) and (b) The separate multipolar contributions n to the scattered field $\mathcal{E}_s$ for the two resonant energies of Fig. 5, for an ellipsoid of $a/b=0.9$ and $b=50$ nm. The angle θ is measured from the z axis in the x-z plane.

of the elementary fields (Ψ_n) as a function of n for the two eccentricities considered. Figure 4(a) is for $a/b=0.9$, and $b=5$ nm, at $E=2.5$ eV ($\lambda=496$ nm), an off-resonance energy, and at $E=3.45$ eV the resonant energy. Calculations at the resonant energies have a slower convergence than those for off-resonant energies. Figure 4(b) shows the same behavior for a higher eccentricity $a/b=0.8$, albeit with a slower convergence.

2. *Electrodynamic regime*

Few calculations have been done to determine local fields in the electrodynamic regime for ellipsoidal particles.[13] The T matrix formalism is ideally suited for this type of calculation and is not restricted to calculation of the local field at the surface of the scatterer as is the case in Ref. 13. Figure 5 shows the result of a T matrix calculation for the spectral dependence of the intensity of the total electric field at the point of highest field intensity for an ellipsoid with $a/b=0.9$ and $b=50$ nm, corresponding to a scatterer in the electrodynamic regime excited by a plane wave whose field is parallel to the major symmetry axis.

A similar analysis to that used for the electrodynamic sphere applied to the resonant peak for an ellipsoid at the point where the maximum value of the field intensity is located permits the identification of the peak as dominantly dipolar in nature, while the other resonant peak to its left is mainly quadrupolar in character. Figure 6 illustrates the multipolar analysis of the scattered field as a function of angle, which corroborates the above assignment of peaks to specific multipoles.

As it also occurs in the case of spheres, the maximum intensity in the electrodynamic case (here $|\mathcal{E}_t|^2=88.4$, $a/b=0.9$, and $b=50$ nm, Fig. 5) is smaller than the maximum intensity for the long-wavelength case (in our calculations $|\mathcal{E}_t|^2=762$ at the tip of an $a/b=0.9$, $b=5$ nm ellipsoid).

II. CLUSTERS

A. The formalism

The T-matrix formalism has been extended to systems with more than one scatterer by Peterson and Ström[14] using the translation theorems for the vector spherical functions.[24] The translation properties of Ψ_n and $\mathrm{Re}\Psi_n$ are summarized by Ref. 25:

$$\mathrm{Re}\Psi_{\tau n}(\mathbf{r}+\mathbf{a})=\sum_{\tau',n'} R_{\tau n,\tau' n'}(\mathbf{a})\mathrm{Re}\Psi_{\tau' n'}(\mathbf{r}) ,$$

$$\Psi_{\tau n}(\mathbf{r}+\mathbf{a})=\sum_{\tau',n'} \sigma_{\tau n,\tau' n'}(\mathbf{a})\mathrm{Re}\Psi_{\tau' n'}(\mathbf{r}) , \quad |\mathbf{a}|>|\mathbf{r}|$$

$$=\sum_{\tau',n'} R_{\tau n,\tau' n'}(\mathbf{a})\Psi_{\tau' n'}(\mathbf{r}) , \quad |\mathbf{a}|<|\mathbf{r}|$$

where $\sigma_{\tau n,\tau' n'}$ and $R_{\tau n,\tau' n'}$ are the elements of the translation matrices as defined in Ref. 14.

Peterson and Ström obtained a T matrix for the cluster of two particles in terms of the T matrices of each single scatterer:

$$\underline{T}(1,2)=\underline{R}(\mathbf{a}_1)\{\underline{T}(1)[\underline{1}-\underline{\sigma}(-\mathbf{a}_1+\mathbf{a}_2)\underline{T}(2)\underline{\sigma}(-\mathbf{a}_2+\mathbf{a}_1)\underline{T}(1)]^{-1}[\underline{1}+\underline{\sigma}(-\mathbf{a}_1+\mathbf{a}_2)\underline{T}(2)\underline{R}(\mathbf{a}_1-\mathbf{a}_2)]\}\underline{R}(-\mathbf{a}_1)$$
$$+\underline{R}(\mathbf{a}_2)\{\underline{T}(2)[\underline{1}-\underline{\sigma}(-\mathbf{a}_2+\mathbf{a}_1)\underline{T}(1)\underline{\sigma}(-\mathbf{a}_1+\mathbf{a}_2)\underline{T}(2)]^{-1}[\underline{1}+\underline{\sigma}(-\mathbf{a}_2+\mathbf{a}_1)\underline{T}(1)\underline{R}(\mathbf{a}_2-\mathbf{a}_1)]\}\underline{R}(-\mathbf{a}_2) ,$$

where $\mathbf{a}_1$ and $\mathbf{a}_2$ are the distances from the origin to the center of each scatterer. As is the case for single scatterers, the calculation of the local fields for clusters are restricted to the exterior of a minimum circumscribing sphere that contains both particles in order to assure convergence of the field expansions.

The above expression for the T matrix of the two-scatterer cluster was obtained by generalizing the formalism from the continuous surface of a single scatterer to the discontinuous surface represented by two distinct scattering sources. This approach can be reduced to a multiple-scattering formulation of the problem by expanding the inverse matrix into a series expansion of the form

$$[\underline{1}-\underline{\sigma}\,\underline{T}\,\underline{\sigma}\,\underline{T}]^{-1}=\underline{1}+[\underline{\sigma}\,\underline{T}\,\underline{\sigma}\,\underline{T}]+[\underline{\sigma}\,\underline{T}\,\underline{\sigma}\,\underline{T}]^2+\cdots ,$$

where the terms of the expansion correspond to different multiple-scattering processes.[14] However, even when the inverse matrix exists, this expansion is not valid when the scatterers are too close to each other, as the authors have verified through several computer calculations, thus making the multiple-scattering representation invalid in this case.

The intensity of the local field in all clusters in this article are calculated at the point where the metallic scatterers touch the minimum circumscribing sphere, a point where the largest enhancement of the local scattered field is usually found.

The method requires the use of computers with large memory capacity and fast processing of data. For this article a "minisupercomputer" with vectorization and parallel-processing capabilities was used.

B. Cluster of two spheres

1. Long-wavelength regime

Recent works about light dispersion by clusters of spheres only take into account particles in the long-wavelength regime using an electrostatic approach,[16,26] and for those done in the electrodynamic regime the scattered field is calculated in the radiation zone.[14]

In contrast to the isolated sphere, it is found that as two spheres approach each other multipolar terms have to be considered even in the long-wavelength regime where the wavelength is much bigger than the size of the scattering cluster. This behavior is explained by the fact that each sphere is immersed in the distorted incident field produced by the other sphere, thus making them respond to other multipoles higher than the dipolar term in the incident field.

Calculations of the intensity of the total field as a function of interparticle distance give the maximum when the spheres are slightly separated from each other. The distance at which the maximum intensity is found will be referred to from here on as the critical distance Δ. Figure 7 shows the intensity of the total field at the trip of the cluster as a function of incident wavelength for various separation distances between the spheres of 5-nm radii (long-wavelength regime). As above, all calculations are performed taking the intensity of the incident electric

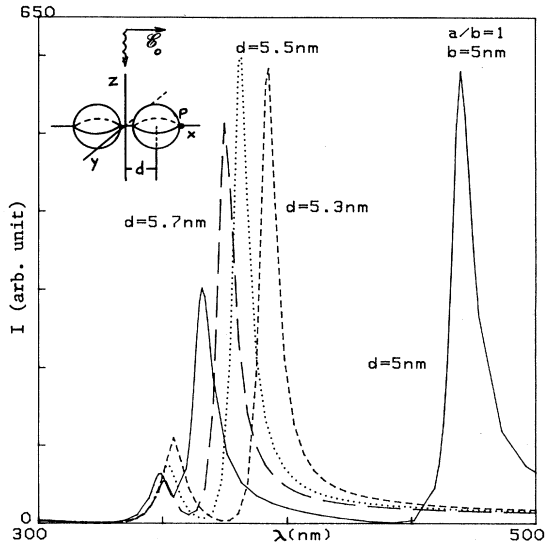

FIG. 7. Total electric field intensity at the point P for a cluster of electrostatic spheres, $a/b=1$ and $b=5$ nm, as a function of incident wavelength. Four distances between the spheres are presented ($d=5$, 5.3, 5.5, and 5.7 nm; $2d$ is the distance between the centers of the particles).

field vector as 1. The maximum intensity enhancement for this specific case is 1.14 times the intensity of the electric field of the single sphere, or 592 times the intensity of the incident wave. Two more peaks are observed due to the clustering process when the spheres touch each other. For all other cases, only two peaks are observed, in accordance with other recent works.[26]

In general, the behavior of the resonant peaks as the distance between spheres increases is to move towards higher energies (smaller wavelengths), in accordance with previous works,[15] reaching the single-sphere resonant energy for distances between the centers of the particles greater than four radii.

Computationally, as the distance between scatterers is increased, more terms have to be considered when the scattered local field is calculated due to the nature of the translation matrices; therefore a bigger matrix has to be taken into account to achieve good results. Nevertheless, the computational capacity available to the authors permitted the obtention of good results up to the decoupling distance mentioned above; for greater distances, the results for the single spheres can be used to calculate local scattered fields. In this article the decoupling distance δ is defined as the distance between the centers of the spheres where the resonant energy, as well as the intensity of the local scattered field coincides with that of the single sphere; that is, if a sphere is separated farther than the decoupling distance δ, the contribution to the local scattered field near one sphere due to the other sphere is negligible. Also, the existence of a decoupling distance permits the considerations of clusters with more than two particles if the higher cluster can be grouped into systems

of two interacting particle clusters.

While for local fields the sizes of the matrices to be considered have to be rather large, for calculations of the scattered field in the radiation zone higher multipolar contributions to the scattered field are no longer important and calculations converge quickly for a large range of interparticle distances within a cluster,[14] as is also the case for single scatterers.

For the case of a single scatterer in the long-wavelength regime the T-matrix formalism can be made to correspond exactly to Claro's[19] electrostatic multipolar expansion. Since his formalism for two-particle clusters is an expansion in multipolar interaction terms that is essentially equivalent to a multiple-scattering formalism, the inverse matrix $[\underline{1}-\underline{\sigma}\,\underline{T}\,\underline{\sigma}\,\underline{T}]^{-1}$ in the theory used by the authors was expanded in a multiple-scattering representation and compared with Claro's result. This multiple-scattering expansion was applied to cluster of spheres in the long-wavelength regime (radius $a=5$ nm) as a function of interparticle distance, obtaining the same divergences observed by Claro for close proximity of the spheres. Thus, it is apparent that the divergences of Claro are due to the multiple-scattering nature of his calculation, an expansion that is not used in this paper. Other electrostatic calculations for clusters of spheres, like those from Ref. 27, do not report divergences when the spheres are in contact, and they coincide with those of the present authors in calculating the inverses of their matrices numerically and not by using the formal expansion of the inverse. Also, the highest-order multipoles n at which the infinite matrices are truncated to obtain adequate results in Ref. 27 coincide with those of the authors in the long-wavelength regime.

Thus, it can be concluded that in the long-wavelength regime, for clusters of two spheres in close proximity ($d/a<1.1$), the multiple-scattering interpretation is no longer valid. This is due to the fact that in these systems the scatterers become strongly coupled when in close proximity, and therefore cannot be thought of as a two-distinct-component system, but as a single more complex scatterer.

Also, the T matrix calculations have been compared with experimental data for clusters of spheres in the electrostatic regime: the real part of the calculated dielectric function corresponding to the resonant energy of a cluster of touching spheres gives a value of -8.23 (using the data from Ref. 20) compared with the experimental value of -3.73 given in Ref. 28. The calculations done by Claro yield an infinite value for the same calculation.[19]

2. *Electrodynamic regime*

As expected, an increase in the size of the spheres will result in a more significant contribution from multipolar terms, reflected in the more intense peaks in the higher-energy part of the spectrum. Figure 8 shows the calculated total electric field intensity as a function of wavelength for the case of a cluster of touching electrodynamic spheres (radius 50 nm) for various distances of observation. In this case three peaks are observed, in contrast with only two for the isolated sphere. Also, comparing

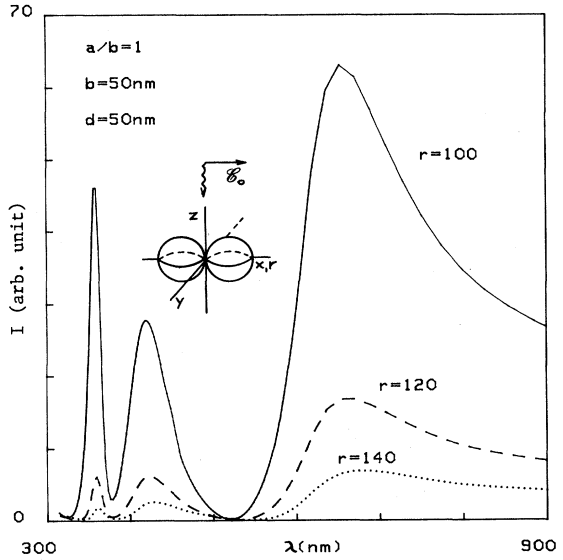

FIG. 8. Total electric field intensity as a function of incident wavelength for a cluster of electrodynamic spheres, $a/b=1$ and $b=50$ nm, with $d=50$ nm. Three distances of observation are presented ($r=100$, 120, and 140 nm). The observation point is on the x axis.

this figure with Fig. 7, $d=5$ nm, the highest-energy peak of the electrodynamic cluster is of comparable intensity to the maximum peak, while for the long-wavelength cluster the highest-energy peak is of negligible size compared to the maximum peak. The maximum intensity of the electric field is 1.01 times the intensity of the electric field around the single sphere and 64 times the intensity of the electric field of the incident wave. As with the case of single spheres, an increase in the size of the scatterers results in a decrease in the enhancement of the field. Convergence to within 5% of the asymptotic value of the field is achieved between $n=10$ and $n=11$ for spheres of this radius.

As argued before in the case of a single ellipsoid, the nonsphericity of the cluster of the two spheres gives rise to nondiagonal terms in the T matrix. As a result, an analysis similar to that followed for single spheres and ellipsoids indicate that it is not possible to assign a specific multipolar nature to each peak, since each is composed of several multipoles that contribute about equally to the local-field strength. Figures 9(a), 9(b), and 9(c) show the magnitude of the total field (all n's considered) as a function of angular position for the resonant energies of the peaks of the cluster of touching electrodynamic spheres. In the three resonant energies considered, the focusing point of energy is mainly in the x axis.

C. Cluster of two prolate spheroids

1. *Long-wavelength regime*

The calculations for clusters of prolate spheroids yield spectral behavior similar to that found for clusters of

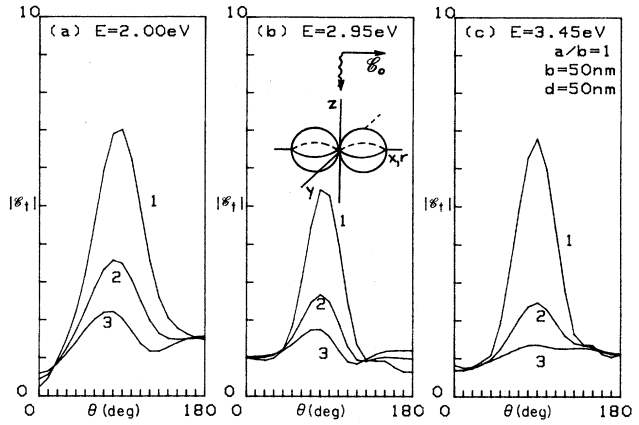

FIG. 9. (a)–(c) Magnitudes of the total electric field $\mathcal{E}_t$ for a cluster of electrodynamic spheres, $a/b=1$ and $b=50$ nm, with $d=50$ nm, as a function of the angle measured from the z axis on the x-z plane. The three energies correspond to the resonances of Fig. 8. Labels 1, 2, and 3 correspond to $r=100$, 120, 140 nm, respectively.

spheres as a function of distance between scatterers. Figures 10(a) and 10(b) show the intensities of the total field around two clusters of prolate spheroids as a function of distance between the particles. Due to computer-time and memory-space limitations, only two cases in the long-wavelength regime are presented, $a/b=0.9$ and $a/b=0.8$, $b=5$ nm. As the distance between the particles is increased in Fig. 10(a), the maximum intensity of the field is found when the spheroids are at a distance of $\Delta=5$ nm [$|\mathcal{E}_t|^2=408$, $d=4.5$ nm, touching case; $|\mathcal{E}_t|^2=483$, $d=5$ nm (both with $a/b=0.9$, $b=5$ nm)]. Figure 10(b) shows an overall decrease in the field intensity compared with Fig. 10(a). The maximum intensity is found at a distance $\Delta=4.75$ nm [$|\mathcal{E}_t|^2=196$, $d=4$ nm, touching case; $|\mathcal{E}_t|^2=271$, $d=4.75$ nm (both with $a/b=0.8$, $b=5$ nm)]. Other calculations done by the authors[29] for ratios $a/b=0.5$ and $b=10$ nm, although approximate because computer power did not permit an exact calculation, also give evidence of the existence of a critical distance Δ greater than the touching distance.

In contrast with the previous behavior shown by the sphere cluster as well as the ellipsoidal clusters, a change of configuration can eliminate the critical distance. Figure 11 shows the intensity of the total field of a cluster of prolate spheroids with their semimajor axis aligned with the x axis, $a/b=0.9$ and $b=5$ nm. The maximum intensity is found when the ellipsoids are touching ($|\mathcal{E}_t|^2=1407$, $d=5$ nm; $a/b=0.9$, $b=5$ nm). Its intensity is higher than the intensity found in the cluster of the same a/b ratio but with the semimajor axis aligned parallel to the z axis (from Fig. 10(a) $|\mathcal{E}_t|^2=483$). This is an expected result since the cluster of spheroids aligned along the x axis forms a system more elongated than the cluster of spheroids aligned along the z axis.

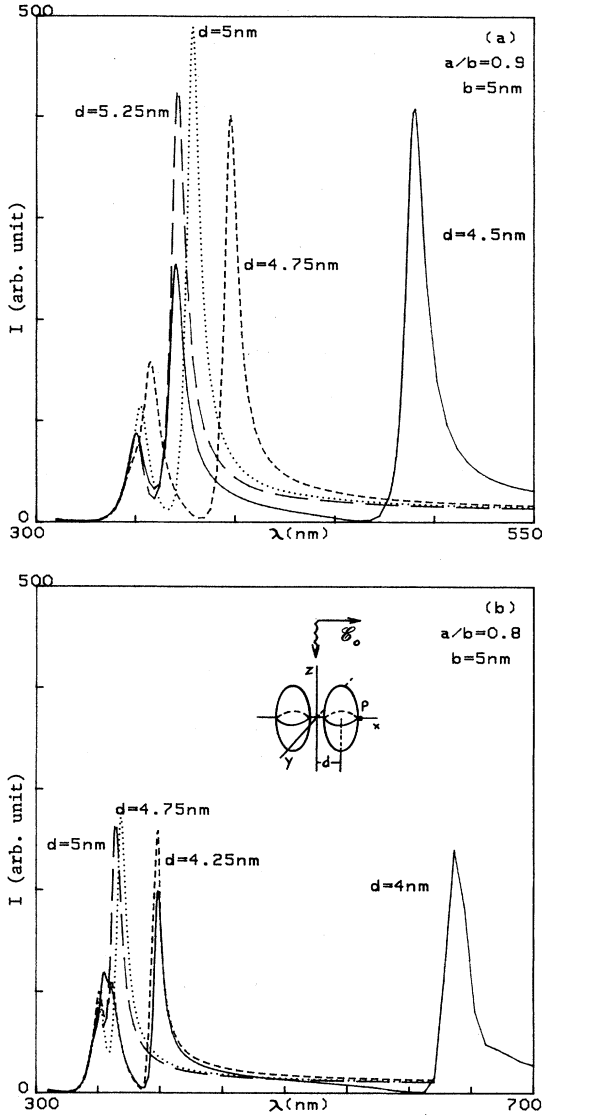

FIG. 10. (a) and (b) Total electric field intensity $|\mathcal{E}_t|^2$ as a function of incident wavelength for four separation distances. Two a/b ratios are presented, (a) $a/b=0.9$, $b=5$ nm; (b) $a/b=0.8$, $b=5$ nm. Point P is the observation point.

2. *Electrodynamic regime*

Calculations for an electrodynamic cluster of spheroids with $a/b=0.9$ and $b=50$ nm are presented in Fig. 12. The following points can be concluded by comparing this figure with the electrodynamic cluster of spheres with $a/b=1$ and $b=50$ nm (Fig. 8): the higher-energy peak is comparable to the lower-energy peak for the cluster of electrodynamic spheres, while for the cluster of electrodynamic ellipsoids it is of less importance; the intensity of the lower-energy peak is higher for the case of the ellipsoids than for the case of the spheres.

The fact that the higher-energy peak is of less importance, compared to the lower-energy one, indicates that

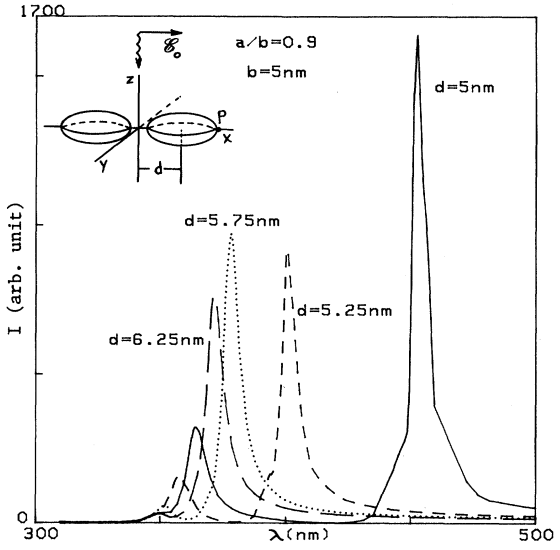

FIG. 11. Total electric field intensity $|\mathcal{E}_t|^2$ as a function of incident wavelength for a cluster of ellipsoids that are aligned along the x axis; $a/b=0.9$ and $b=5$ nm for four distances of separation. Point P is the observation point.

the geometrical configuration of the two ellipsoids inhibit multipoles with high-energy resonances, while for the case of the spheres (Fig. 8) the configuration favors high-energy multipoles. The fact that the intensity of the peak increases ($|\mathcal{E}|^2=63$ for electrodynamic spheres, $|\mathcal{E}|^2=82$ for electrodynamic ellipsoids) can be explained considering that more eccentric scatterers tend to concentrate the scattered local field in a particular direction because of the antenna effect.

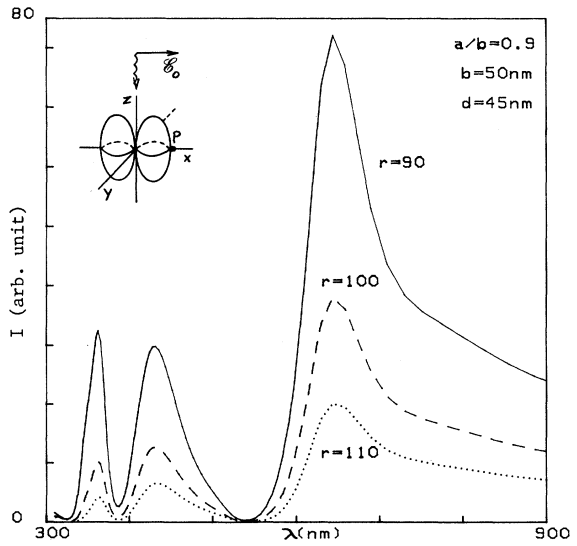

FIG. 12. Total electric field intensity $|\mathcal{E}_t|^2$ as a function of incident wavelength for an electrodynamic cluster, $a/b=0.9$ and $b=50$ nm. Three distances of observation are presented ($r=90$, 100, and 110 nm). The observation point P is shown in the diagram.

In similitude to the case of the cluster of electrodynamic spheres, the resonant peaks of the cluster of electrodynamic ellipsoids cannot be characterized by a dominant multipolar contribution since the strongly nondiagonal nature of the T matrix tends to mix many multipoles into the composition of each resonant peak.

CONCLUSIONS

The T matrix formalism of Waterman was applied to the calculation of the local electric fields near a single metallic scatterer as well as clusters of two scatterers, both in the long-wavelength and the electrodynamic regimes.

For the case of single spheres, the formalism becomes equivalent to the Mie theory and calculations in the electrodynamic regime for a single spherical scatterer agree with work done by other authors. The scattered-field behavior as a function of observation distance r reduces to pure dipolar behavior for $r\approx 2a$. A procedure for characterizing the multipolar nature of the resonance peaks for ellipsoids as well as for clusters in the long-wavelengths regime was established.

Increase in size, as well as decrease in a/b ratio of ellipsoids and proximity to a resonance, requires the consideration of higher multipoles to obtain local fields, thus making the dipolar approximations invalid. The rates of decay of these fields as a function of the distances from the scatterers are easily calculated with the T matrix approach and it is possible to assign the multipolar character of all resonances. Furthermore, the enhancement effect of the local electric field diminishes with increasing size of the single scatterers. More specifically, we find that in ellipsoids, for $\lambda \gg b$ and $r \cong b$, higher multipolar contributions must be included: therefore, in order to get a good convergence, more terms have to be considered as the eccentricities increase, while for $\lambda \gg b$ and $r \gg b$ higher multipoles contribute marginally and the dipolar approximation becomes valid.

The study of clusters with the T-matrix method has made possible comparison of results with recent electrostatic approaches as well as the calculation of local electric fields for clusters in the electrodynamic regime. The analysis of a multiple-scattering expansions in the long-wavelength regime and comparison with published results[19] indicates that for clusters in close proximity ($d/a<1.1$) this type of expansion is no longer valid due to the strong interaction between the two scattering sources in the cluster.

Electric field intensities around clusters are greater in magnitude compared to the intensities for the corresponding isolated particles, indicating the capacity of the clusters to localize spatially the field intensity, which suggests that for any calculation of enhanced Raman scattering, it is necessary to consider clustering effects.

For the cases of electric field intensity as a function of separation between particles, a critical distance Δ greater than the one corresponding to touching scatterers is found for most of the cases studied. The existence of this

critical distance is probably due to the complex angular dependence of higher multipoles. The fact that higher multipoles have a greater degree of anisotropy affords the possibility that the field generated by each of the individual scatterers will result in a net field that has a maximum for interparticle distances larger than when the scatterers touch each other.

Therefore, we conclude that to obtain the greatest enhancement of the intensity of the scattered electric field in granular materials, two fundamental lengths have to be considered. One due to long-range correlation length that is important in predicting the effective optical dielectric function of the material as a whole, as shown by the authors elsewhere.[30] The other, short range in nature, corresponding to the mean distance between nearest-neighbor granules, which is related to the contribution of clustering effects to the local-field enhancement. The long-range-order correlation length describes the statistical correlation between the position of the particles that is determined by the formation process of the granular material. The short-range-order length is related to the average distance between islands and is dependent on the concentration of the constituent materials.

For clusters, accuracy is harder to obtain, computational time increases, and more memory space is needed, but good results are still obtained with available computational resources up to the decoupling distance $\delta \geq 4a$ for spherical and ellipsoidal scatterers in both long-wavelength and electrodynamic regimes. This will permit the use of simplifying assumptions in the calculation of local-field clusters of more than two scattering sources.

In conclusion, the T-matrix formalism has proven to be a strong calculational technique for studying the local field near clusters of metallic particles and arbitrary shaped scatterers taking into account multipolar as well as retardation effects. The authors are in the process of extending the calculation to three-scatterer clusters, and arbitrarily oriented ellipsoids within a cluster, and the application of this result to the study of enhanced Raman scattering.

ACKNOWLEDGMENTS

This work was supported by the National Science Foundation (under Grant No. INT-85-09185) and partially supported by the United States Army Research Office (under Grant No. DAAG-29-84-G-0059).

[1]Lord Rayleigh, Proc. R. Soc. London, Ser. A **84**, 25 (1910).
[2]G. Mie, Ann. Phys. (Leipzig) **25**, 377 (1908).
[3]R. P. Devatty and A. J. Sievers, Phys. Rev. B **24**, 1079 (1981).
[4]J. M. Calleja and F. Agullo-Lopez, J. Phys. Chem. Solids **37**, 363 (1976).
[5]E. Rzepka, L. Taurel, and S. Lefrant, Surf. Sci. **106**, 345 (1981).
[6]M. Moskovits, Rev. Mod. Phys. **57**, 783 (1985).
[7]H. Reimer, F. Fischer, Phys. Status Solidi B **124**, 61 (1984).
[8]W. Kleeman, Z. Phys. **215**, 113 (1968).
[9]P. C. Waterman, Phys. Rev. D **3**, 825 (1971).
[10]D. S. Wang and M. Kerker, Phys. Rev. B **24**, 1777 (1981).
[11]P. Barber and C. Yeh, Appl. Opt. **14**, 2864 (1975).
[12]H. Chew, D. S. Wang, and M. Kerker, J. Opt. Soc. Am. B **1**, 56 (1984).
[13]P. W. Barber, R. K. Chang, and H. Massoudi, Phys. Rev. B **27**, 7251 (1983).
[14]B. Peterson and S. Ström, Phys. Rev. D **8**, 3661 (1973).
[15]F. Claro, Phys. Rev. B **30**, 4989 (1984).
[16]R. Fuchs and F. Claro, Phys. Rev. B **35**, 3722 (1987).
[17]Z. Chen, P. Sheng, D. A. Weitz, H. M. Lindsay, M. Y. Lin, and P. Meakin, Phys. Rev. B **37**, 5232 (1988).
[18]See, for example, Refs. 26 and 27 and references therein.
[19]F. Claro, Phys. Rev. B **25**, 2483 (1982).
[20]P. B. Johnson and R. W. Christy, Phys. Rev. B **6**, 4370 (1972).
[21]J. A. Stratton, *Electromagnetic Theory* (McGraw-Hill, New York, 1941), p. 212.
[22]S. S. Martinos, Phys. Rev. B **31**, 2029 (1985).
[23]B. J. Messinger, K. U. von Raben, R. K. Chang, and P. W. Barber, Phys. Rev. B **24**, 649 (1981).
[24]O. R. Cruzan, Q. Appl. Math. **20**, 33 (1962).
[25]V. K. Varadan and V. V. Varadan, *International Symposium on: Acoustic, Electromagnetic, and Elastic Wave Scattering—Focus on the T-matrix Approach* (Pergamon, New York, 1979), p. 48.
[26]N. Liver, A. Nitzan, and J. I. Gersten, Chem. Phys. Lett. **111**, 449 (1984).
[27]N. Liver, A. Nitzan, and K. F. Freed, J. Chem. Phys. **82**, 3831 (1985).
[28]J. E. Sansonetti and J. K. Furdyna, Phys. Rev. B **22**, 2866 (1980).
[29]M. Gómez, L. Fonseca, and L. Cruz, in *Proceedings of the International Workshop on the Electrodynamics of Interfaces and Composite Systems,* edited by R. G. Barrera and W.L. Mochan (World Scientific, Singapore, 1988).
[30]M. Gómez, L. Fonseca, G. Rodriguez, A. Velazquez, and L. Cruz, Phys. Rev. B **32**, 3429 (1985).